ISSN 1063-7826, Semiconductors, 2016, Vol. 50, No. 2, pp. 171–179. © Pleiades Publishing, Ltd., 2016.
Original Russian Text © A.V. Bakulin, S.E. Kulkova, 2016, published in Fizika i Tekhnika Poluprovodnikov, 2016, Vol. 50, No. 2, pp. 171–179.

SURFACES, INTERFACES, AND THIN FILMS

Halogen Adsorption at an As-Stabilized β2–GaAs (001)–(2 × 4) Surface

A. V. Bakulin[a, b]* and S. E. Kulkova[a, b]

[a] *Institute of Strength Physics and Materials Science, Siberian Branch, Russian Academy of Sciences, Tomsk, 634055 Russia*
[b] *National Research Tomsk State University, Tomsk, 634050 Russia*
**e-mail: bakulin@ispms.tsc.ru*

Submitted June 16, 2015; accepted for publication June 18, 2015

Abstract—Halogen (F, Cl, Br, and I) adsorption at an As-stabilized GaAs (001) surface with the β2–(2 × 4) reconstruction is studied using the plane-wave projected-augmented wave method. The effect of halogens on the structural and electronic characteristics of the semiconductor surface is analyzed. The T_2' site at the missing row edge is shown to be the energetically most favorable for the adsorption of F, Cl, and Br, whereas I prefers the H_3 site between adjacent arsenic dimers in the third layer from the surface. Ga-halogen bond formation suggests that charge is transferred via the depletion of occupied orbitals of the As-dimer surface atoms, which leads to the weakening of Ga–As bonds in the substrate. The weakening of bonds between substrate-surface atoms due to the interaction of halogens with the surface is estimated.

DOI: 10.1134/S1063782616020056

1. INTRODUCTION

Keen interest in studying the atomic and electronic structure of $A^{III}B^{V}$ semiconductors and low-dimensional systems based on them over the last few decades is due to by the wide application of these materials in microelectronics, spintronics, and in optical and magnetic devices. The progress in modern nanotechnologies assumes the development of methods for controlling the structure and properties of the surface of semiconductor compounds at the atomic scale, which is impossible without an understanding of the mechanisms of interaction between different adsorbates and the surface, depending on the chemical composition of the latter. This stimulates interest in theoretical investigations of the surface electronic structure of semiconductor materials with the use of ab initio techniques. The level of development of modern computer equipment and program codes for the implementation of these techniques allows correct calculations of the total energy for forming surface structures, forces on surface atoms, surface relaxation, geometry of adsorbates, and their binding energy to the surface.

It is well-known that the electronic properties of $A^{III}B^{V}$ semiconductor surfaces depend on their orientation, structure, the presence of defects, and adsorbed atoms [1–4]. The largest variety of surface structures was found for the polar $A^{III}B^{V}(001)$ surface. Although the structural and electronic properties of different reconstructions of this surface have been investigated over the last few decades (see, for example, [2, 3, 5] and references therein), many surface reconstructions remain debatable. The latter complicates interpretation of the interaction between adsorbates and semiconductor surfaces, which is necessary for developing techniques of atomic layer or "digital" etching of a semiconductor surface, allowing atomic layers and even individual atoms to be removed in a controlled way with an atomically smooth surface retained. In binary $A^{III}B^{V}$ compounds, atomic-layer etching is performed with the use of halogens or halogen-containing molecules [4]; however, the effect of halogens on the interatomic bonds in surface layers is still unclear. In our previous studies [6–9], we investigated the interaction of halogens with cation-rich GaAs (001) and InAs (001) surfaces. We demonstrated that, regardless of the type of surface reconstruction, within the cation-rich limit halogens prefer to form bonds mainly with cation surface atoms. This leads to halogen-induced charge-density redistribution between anion and cation surface atoms, as well as to the weakening of bonds between cation atoms and the substrate, which is the first stage in the etching of a cation-rich semiconductor surface. In the anion-rich region on the $A^{III}B^{V}$ (001) surface, the stable reconstruction is β2–(2 × 4) [2] and in this region is the only site where halogens can interact with a cation of the second layer from the surface. The interaction of halogens with the anion-rich $A^{III}B^{V}$ (001) surface was experimentally investigated in [10–12]. It was concluded that halogen adsorption can lead to surface disordering. Since halogen adsorption in the case of

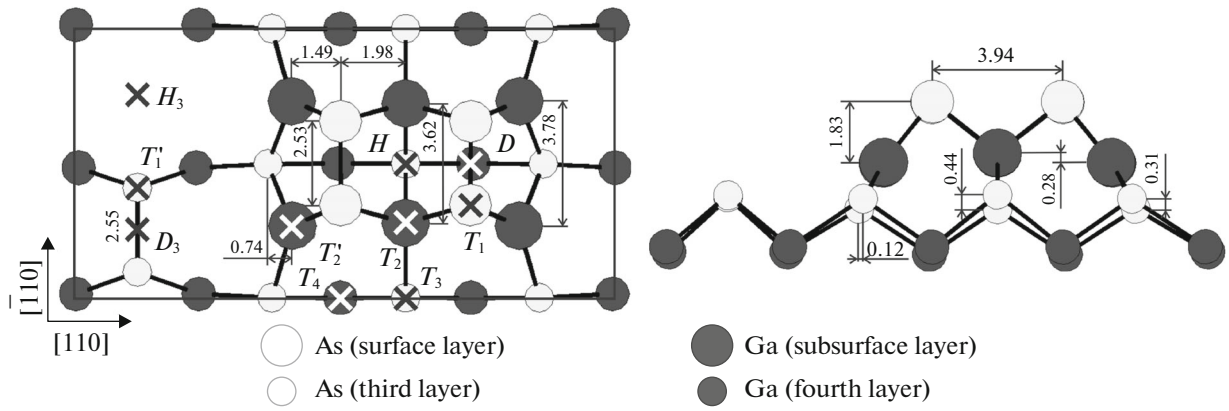

Fig. 1. Atomic structure of the surface (top view) and halogen-adsorption sites (crosses) on the β2–GaAs (001)–(2 × 4) surface. Gallium and arsenic atoms are shown by closed and open circles, respectively.

the β2–(2 × 4) reconstruction has not been studied yet, it is of interest to establish the trends in the mechanism of the chemical bonding of halogens on a surface of this type.

In this study, we systematically investigate the interaction of halogens (F, Cl, Br, and I) with an As-stabilized GaAs (001) surface and reveal their effect on the structural and electronic characteristics of this surface.

2. CALCULATION TECHNIQUE

The atomic and electronic structures of a GaAs (001) surface with the β2–(2 × 4) reconstruction were calculated by the projected augmented-wave (PAW) method with a plane-wave basis [13, 14], implemented by the VASP software package [15, 16] with the generalized gradient approximation (GGA) for the exchange-correlation functional [17]. The obtained theoretical GaAs lattice parameter is 5.76 Å, which agrees well with a value of 5.78 Å from [18], although it exceeds the experimental parameter 5.65 Å [19]. In the present calculation of the (2 × 4) surface semiconductor structure, we used the theoretical parameter for the bulk material; the surface cell dimensions were $a\sqrt{2} \times 2a\sqrt{2}$. The β2–GaAs (001)–(2 × 4) surface was simulated by seven-layer films separated by ~10 Å vacuum gaps. The surface terminated with arsenic was saturated by pseudo-hydrogen atoms with a fractional charge of 0.75 electrons and, thus, one side of the film was bulk-like [20]. The equilibrium As–H bond length is 1.557 Å. On the other side of the film terminated with gallium, the β2 reconstruction was simulated. Integration over the Brillouin zone was performed using a 6 × 3 × 1 grid of k vectors obtained in accordance with the Monkhorst–Pack scheme [21]. The cutoff of the kinetic energy was 500 eV. The position of two arsenic and gallium atomic layers on one film side saturated by pseudo-hydrogen atoms was fixed at the bulk values, while the position of atoms in the remaining layers was optimized. The atomic structure was relaxed before reaching minimum forces of no larger than 0.01 eV/Å at atoms with the use of the Newtonian dynamics.

The binding energy E_b of halogens to the substrate was calculated from the formula

$$E_b = -[E(\text{halogen/GaAs}) - E(\text{GaAs}) - E(\text{halogen})],$$

where E(halogen/GaAs) and E(GaAs) are the total energies of a system with adsorbed halogen and of a pure surface, and E(halogen) is the halogen-atom energy.

3. RESULTS AND DISCUSSION

3.1. Atomic and Electronic Structure of the β2–GaAs (001)–(2 × 4) Surface

Figure 1 shows the atomic structure of the β2–GaAs (001)–(2 × 4) surface. It can be seen that this reconstruction is characterized by the presence of two arsenic dimers in the surface layer and one arsenic dimer in the third layer from the surface. The calculated bond lengths in the arsenic dimers of the surface layer and third layer from the surface are 2.53 and 2.55 Å, which is slightly larger than the bond lengths in dimers (2.50 and 2.52 Å [22], 2.48 and 2.50 Å [23], and 2.45–2.50 Å [24]) obtained using the local density approximation (LDA). We recall that the GaAs lattice parameter calculated in the LDA is smaller than the experimental value. The spread in the theoretical parameters obtained in the LDA is 5.51–5.63 Å [2, 22–26]. Other interatomic distances characteristic of this structure are presented in Fig. 1. Similar to the above-mentioned bond lengths in arsenic dimers, all the calculated parameters are also somewhat higher than those obtained in the early calculations [22, 24, 27–29], which is due to the use of the GGA approximation for the exchange-correlation functional in the present calculation. In general, the obtained trends in interatomic bond lengths and shifts of surface atoms are consistent with previous calculations with the use of the LDA.

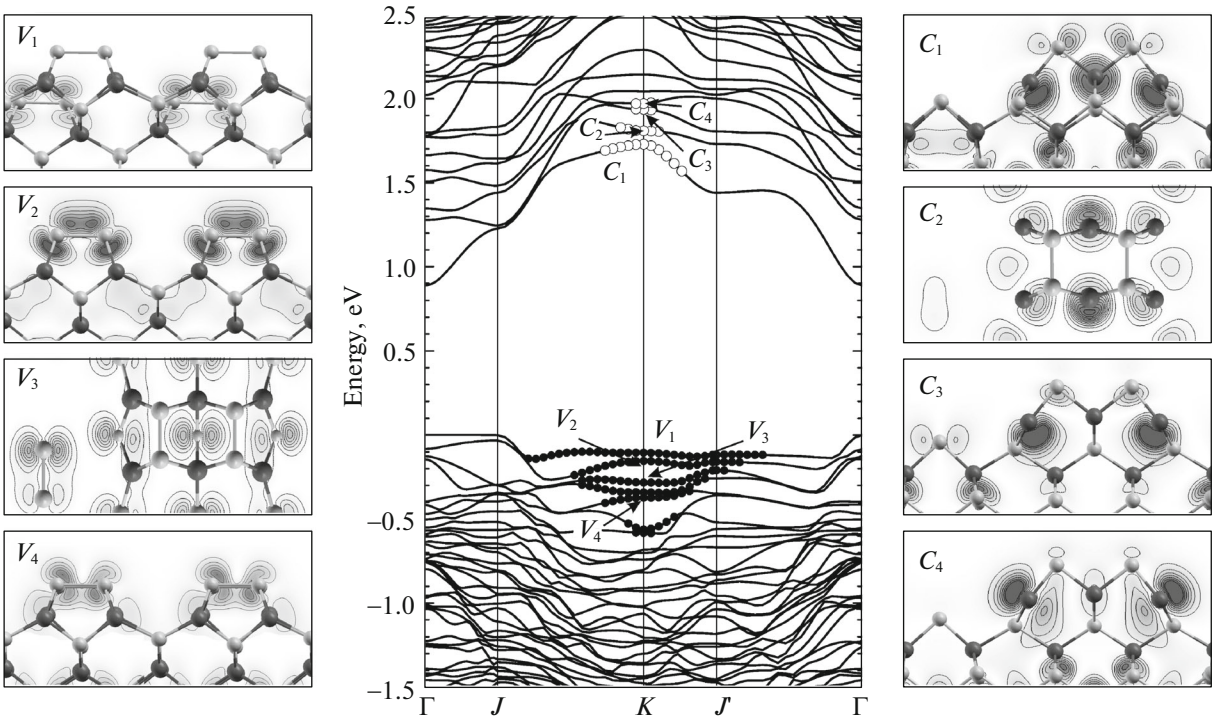

Fig. 2. Electron energy spectrum of the β2–GaAs (001)–(2 × 4) surface and orbital composition of occupied (*V*) and unoccupied (*C*) surface states at point *K* of the 2D Brillouin zone. The top view is shown for states V_3 and C_2 and the side view is shown for the remaining surface states. The occupied and unoccupied surface states are indicated by closed and open circles.

Figure 2 shows the electron energy spectrum of the surface with the β2–(2 × 4) reconstruction and localization of several occupied (*V*) and unoccupied (*C*) surface states. It can be seen that the surface states of the β2–(2 × 4) reconstruction are localized near point *K* of the two-dimensional Brillouin zone. The occupied surface state V_1 is localized at arsenic atoms of the subsurface dimer, but, in contrast to [22], is more widely distributed over the Brillouin zone. The deeper surface state V_2 is localized at dimerized surface arsenic atoms. The state V_3 is caused by orbitals of dimerized and non-dimerized arsenic atoms of the third layer, while the state V_4 is localized at surface arsenic dimers. This is consistent with the conclusion made in [22, 23]. In general, the occupied surface states are localized in the energy range 0.11–0.58 eV below the top of the valence band, as in [22], although in the corresponding publication the surface states were shown schematically.

The unoccupied surface states are mainly localized at gallium atoms of the subsurface layer and the surface state C_1 is slightly contributed to by arsenic atoms of the two surface dimers. It is worth noting that dimer arsenic atoms of the first and second layers also contribute to the state C_3, whereas in [29] it was shown to be caused only by orbitals of dimer atoms of the third layer. Thus, the atomic and electronic structures of a pure As-stabilized GaAs (001) surface with the β2–(2 × 4) reconstruction are correctly reproduced in the PAW-based calculation.

3.2. Halogen Adsorption at the β2–GaAs (001)–(2 × 4) Surface

As can be seen in Fig. 1, the surface with the β2–GaAs (001)–(2 × 4) reconstruction contains mainly adsorption sites where halogen is located near arsenic

Table 1. Binding energy of halogens (in eV) for symmetric sites on the As-stabilized β2–GaAs (001)–(2 × 4) surface

Sites	T_1	T_1'	T_2	T_2'	T_3	T_4	D	H	D_3	H_3
F-GaAs (001)	3.70	4.01	3.06	4.77	3.96	$\rightarrow T_2'$	3.31	3.21	$\rightarrow T_1'$	$\rightarrow T_1'$
Cl-GaAs (001)	1.93	2.27	1.43	2.89	2.03	2.33	1.58	1.53	$\rightarrow T_1'$	2.52
Br-GaAs (001)	1.78	$\rightarrow H_3$	1.36	2.66	1.78	2.29	1.45	1.44	$\rightarrow H_3$	2.48
I-GaAs (001)	1.18	$\rightarrow H_3$	0.83	1.79	1.09	1.67	0.83	0.83	$\rightarrow H_3$	1.87

Table 2. Shift (in Å) of Ga and As surface atoms upon halogen adsorption on the β2–GaAs (001)–(2 × 4) surface relative to their sites on a pure surface

Sites	T_1	T_1'	T_2'
F	–0.032	–0.436	0.251
Cl	–0.014	–0.433	0.306
Br	–0.021	$\rightarrow H_3$	0.309
I	–0.024	$\rightarrow H_3$	0.315

atoms. Since gallium is located in the subsurface layer, all its orbitals are nonreactive, except for gallium in the T_2' site near the missing row edge, where it has a dangling bond. It is worth noting that arsenic atoms of the surface dimers also have nonreactive occupied orbitals. It is considered [10–12] that halogens initially interact with a cation at the T_2' site, which is possibly due to charge redistribution from surface arsenic atoms, and only after that do they interact with arsenic atoms in the surface layer. Below we demonstrate that our calculations generally confirm this pattern.

The calculated binding energies of halogen to the surface for symmetric sites are listed in Table 1. It can be seen that, indeed, F, Cl, and Br have the highest binding energies in the T_2' site above the gallium atom at the missing row edge, while the binding energy of iodine in the T_2' site is lower than in the H_3 site between arsenic atoms of adjacent dimers of the third layer from the surface by only 0.08 eV. We remind that the interaction of halogens with cations at top sites was found to be more preferable at the cation-rich GaAs (001) and InAs (001) surfaces, regardless of their reconstruction, (ζ – (4 × 2), β3' – (4 × 2), or (2 × 4) mixed dimer structure [6–9]. It is worth noting that upon adsorption in the bridge D_3 site above the dimer atoms of the third layer from the surface, iodine repulses dimer arsenic atoms, which leads to the redimerization of arsenic atoms and, then, it actually appears at the H_3 site between two new dimers. The binding energy is also high at the T_4 site, where iodine is located between the arsenic dimers of the first layer. The same trend is observed for chlorine and bromine, whereas fluorine shifts from this site to T_2' upon relaxation. It can be seen from Table 1 that in the remaining sites under consideration the binding energies of halogen with the nearest substrate atoms are significantly lower. It is of interest that fluorine in the missing row prefers to form a bond with one arsenic atom only in the dimer of the third layer from the surface, while the adsorption of chlorine and bromine at the H_3 site in the missing row is energetically more favorable. The adsorption of halogens above surface arsenic dimer atoms is less favorable than in the missing row. Generally, the binding energies of halogen adatoms to an As-stabilized surface are higher for more electronegative halogens and decrease in the series F, Cl, Br, and I, which is consistent with the trends established for a cation-stabilized surface [6–8].

The calculated shifts of surface atoms upon halogen adsorption in top sites are given in Table 2. It can be seen that gallium atoms shift toward vacuum upon halogen adsorption at the T_2' site; the shift of gallium atoms increases with the halogen-adatom covalent radius. At the same time, dimerized arsenic atoms upon halogen adsorption at the T_1 and T_1' sites shift toward the bulk. Similar trends were observed in the case of halogen adsorption above arsenic atoms at the

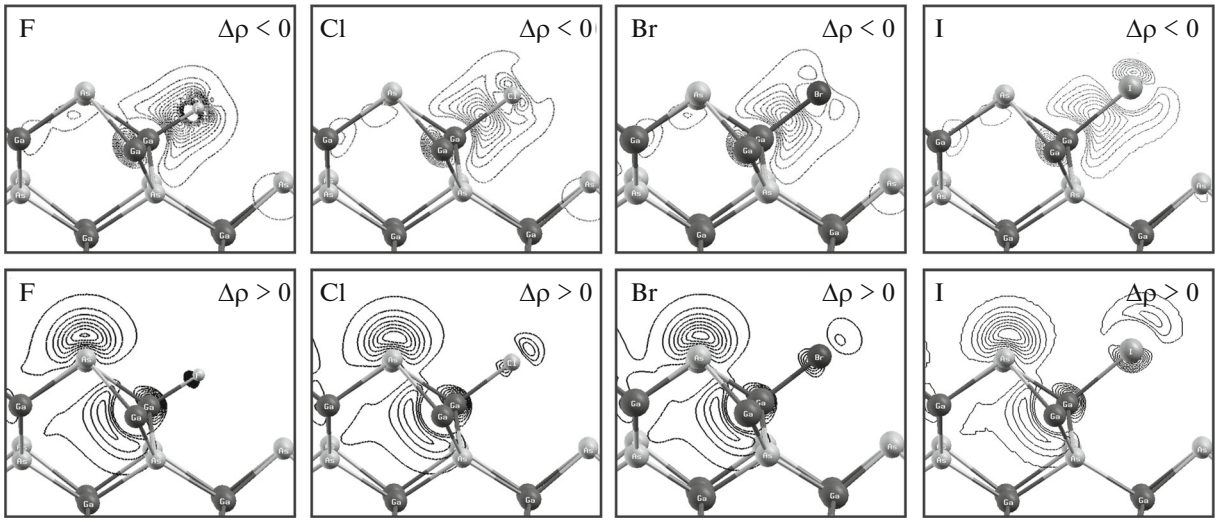

Fig. 3. Charge-density-difference distribution upon halogen adsorption at the T_2' site on the β2–GaAs (001)–(2 × 4) surface: charge accumulation regions (Δρ < 0) are shown at the top and the charge decrease regions (Δρ > 0) are shown at the bottom.

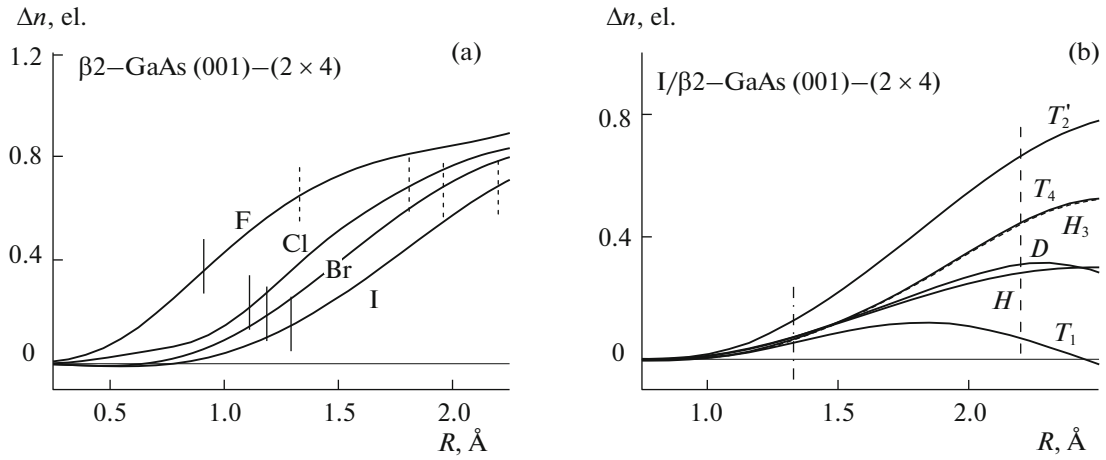

Fig. 4. Difference in the charge density of valence electrons integrated over the sphere as a function of the integration radius (a) for halogens adsorbed at the T_2' site and (b) for iodine on the GaAs (001) surface depending on the adsorption site. Vertical solid lines show the sphere radius equal to a half-length of the bond between the halogen adatom and the substrate. Dashed and dash-dotted vertical lines show the ionic and covalent halogen radii.

missing row edge on the surface with the ζ – (4 × 2) reconstruction. The variation in the position of the surface dimer atoms is less important than that of the arsenic dimer atoms of the third layer from the surface. This is apparently due to the highly preferred halogen adsorption at the T_1' site (Fig. 1), although adsorption at this site is implemented only for fluorine and chlorine, i.e., adsorbates of a smaller size.

Figure 3 shows the charge-density difference $\Delta\rho(r) = \rho_{GaAs}(r) + \rho_{halogen}(r) - \rho_{halogen/GaAs}(r)$ upon halogen adsorption at the missing row edge near gallium atoms of the second layer (T_2' site). We can observe charge accumulation at the gallium–halogen bond, while the charge leaves the nearest surface arsenic dimer atoms. The density of isolines at the Ga–F bond is higher than at the bond between gallium and other halogens, which can indicate a stronger bond between fluorine and the substrate. In this case, we observe the maximum charge transfer from the surface to the halogen (~0.65–0.70*e*) in the case of integration of the charge-density difference over a sphere with a radius equal to the ionic radius of the halogen (Fig. 4a). The charge transferred from the semiconductor substrate to the halogen adsorbed at the T_2' site increases with halogen electronegativity. This can be more clearly seen in the case of integration of the charge-density difference over a sphere equal to half the bond length between a halogen adatom and gallium. These results are shown by solid vertical lines in Fig. 4a. As is known, the charge in the sphere significantly depends on its radius. As shown previously by us [8], the results of integration using the Bader technique [30] in so-called Bader volumes, at the boundaries of which the charge density is minimum, are closer to the results obtained using ionic radii.

The other adsorption sites are characterized by lower charge transfer than at the T_2' site (Fig. 4b). For example, upon iodine adsorption at the H_3 and T_4 sites where the binding energies are high, the charge transfer from the substrate to iodine is ~0.40*e*. Such a charge can be obtained from the tales of the wave functions of halogen adatoms nearest to the adsorption site. In available publications, this charge is referred to as "ghosts" and considered to be not localized at specific atoms.

Figure 5 shows the charge-density-difference distribution upon chlorine adsorption for some other sites at the semiconductor surface. It can be seen that the charge at the H_3 site leaves the bond between the dimer arsenic atoms of the third layer from the surface and is accumulated between atoms of adjacent dimers. A similar picture is observed also for the T_4 sites, but, in this case, the charge leaves the surface arsenic dimers. It is worth noting that, upon chlorine adsorption at the bridge *D* site (not shown in Fig. 5), the charge, as at the H_3 site, leaves the dimer bonds, but is accumulated at the arsenic–chlorine bonds. However, the bond between halogens and arsenic in this site is very weak (Table 1). Upon halogen adsorption at the T_1' site, the opposite trend is observed, i.e., the charge leaves the arsenic–halogen bond and is accumulated at the bond between the dimerized arsenic atom and gallium of the fourth layer; in this case, the arsenic dimer atom above which the halogen is absorbed shifts to the bulk, as was mentioned above. Such a situation was observed for cation-stabilized GaAs (001) and InAs (001) surfaces at the S_7 site [6, 8]. The above-mentioned pattern of the charge-density-difference distribution for a semiconductor with absorbed chlorine remains valid for other halogens at the investi-

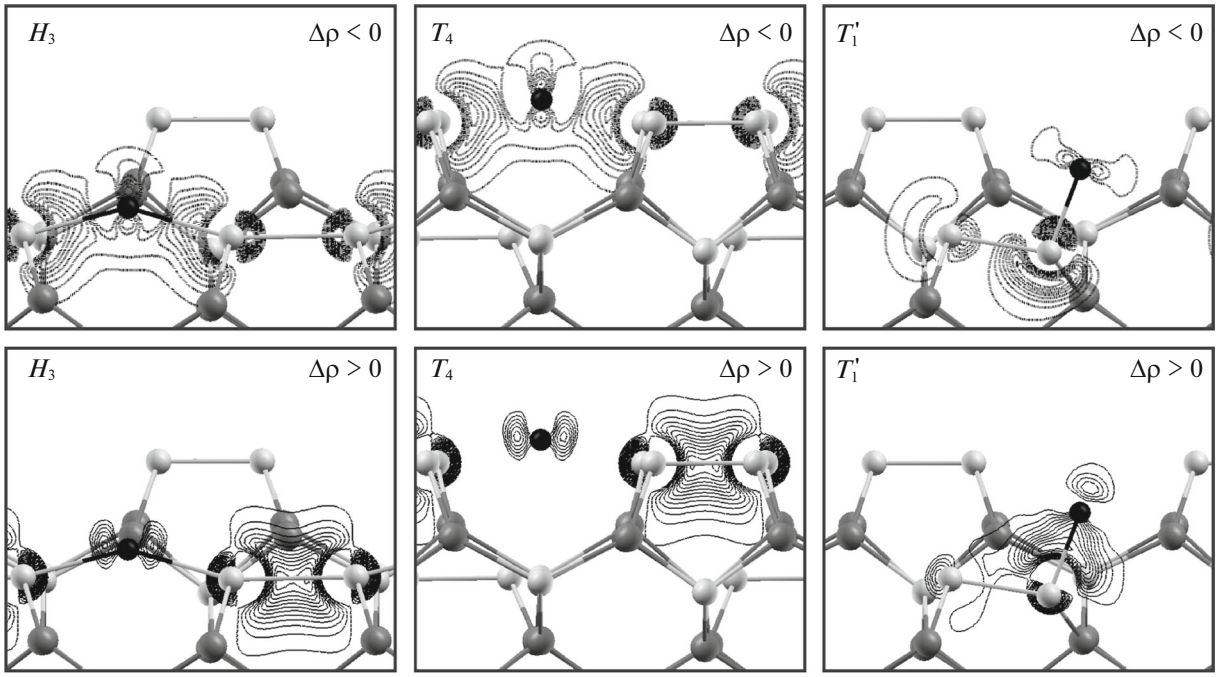

Fig. 5. Charge-density difference for some sites of chlorine adsorbed on the β2–GaAs (001)–(2 × 4) surface: charge accumulation regions ($\Delta\rho < 0$) are shown at the top and the charge decrease regions ($\Delta\rho > 0$) are shown at the bottom.

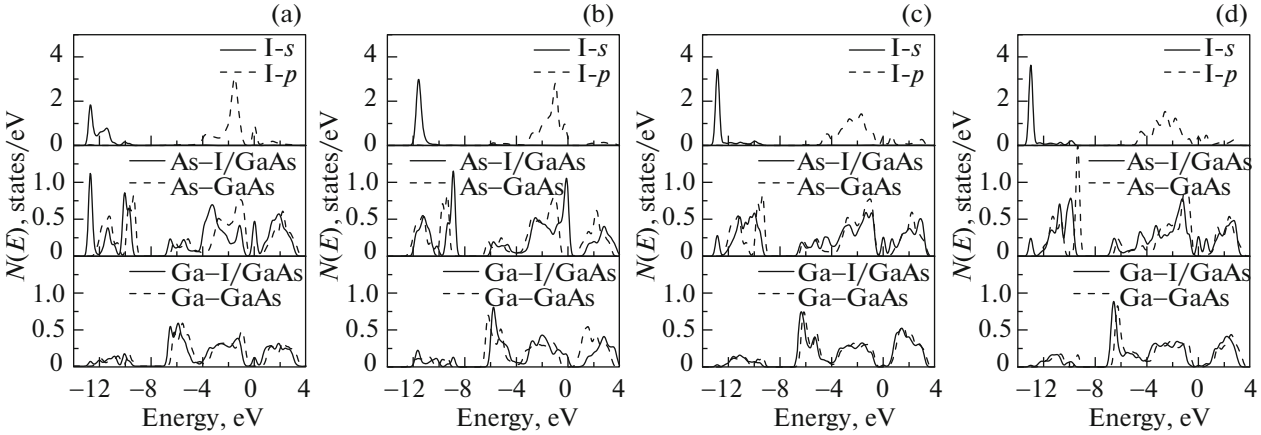

Fig. 6. Local DOSs of iodine and the nearest surface atoms on the β2–GaAs (001)–(2 × 4) surface upon adsorption at (a) the T_1, (b) T_2', (c) T_4, and (d) H_3 sites.

gated adsorption sites. In general, for most of the studied sites at the surface charge redistribution occurs more laterally than upon halogen adsorption at a Ga-stabilized surface.

Analysis of the local electron densities of states (LDOS) for some adsorption sites (Fig. 6) at the β2–GaAs (001)–(2 × 4) surface shows that the states of arsenic atoms change more drastically than those of gallium atoms. Let us discuss the results of the LDOS calculation by the example of iodine. As was mentioned above, at the T_2' site the gallium atom is closest to the adsorbate. The Ga–I bond length is 2.57 Å, while arsenic atoms lie at a distance of 3.96–4.14 Å. At the same time, the gallium states are almost unoccupied. To form a bond with the halogen, the gallium atom requires a charge of ~1e, which can be obtained from arsenic atoms (Fig. 3). In this case, the interaction of the halogen with the arsenic state is indirect and is implemented via the hybridization of arsenic and gallium orbitals. It can be seen in Fig. 6b that the gallium LDOS radically changes due to the hybridization of gallium p states with iodine p states (the region to –4.0 eV below the top of the valence band) and

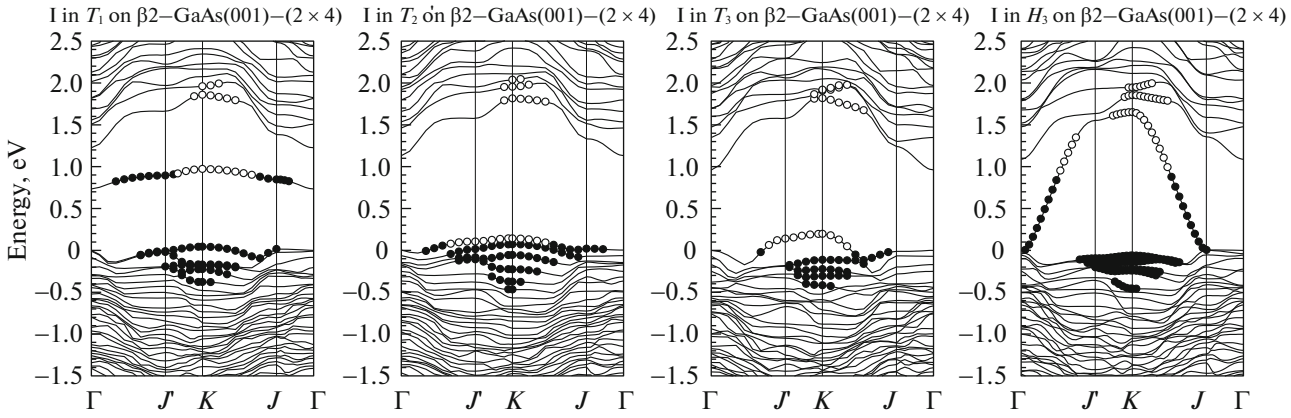

Fig. 7. Electron-energy spectrum of the β2–GaAs (001)–(2 × 4) surface with adsorbed iodine at the T_1, T_2', T_3, and H_3 sites. Closed and open circles show occupied and unoccupied surface states.

depletion of the top of the arsenic valence band. It is worth noting that the iodine states with *s* symmetry are also involved in the interaction with gallium *s* orbitals near –12 eV (Fig. 6b).

At the other sites (H_3, T_4, D, etc.), where the nearest neighbor of iodine is arsenic, the iodine valence states change to a greater extent than do the gallium states (Figs. 6c and 6d). Displacement of the LDOS of arsenic relative to its states at a pure surface and the occurrence of characteristic peaks in the band gap are indicative of the depletion of arsenic states upon halogen adsorption. At the same time, at the T_1 top-site (Fig. 6a) and at the bridge D site, where iodine lies at a distance from gallium atoms of the second layer of ~4.74 Å, the gallium LDOS also undergoes corresponding variations induced by interaction with arsenic orbitals directly in contact with halogen. This is confirmed by the appearance of new peaks in the gallium LDOS, whose positions coincide with the LDOS peaks of arsenic involved in the interaction with the halogen. In general, the pattern of LDOS variation (Fig. 6) is similar to that for the other halogens; however, due to the shift of halogen states toward negative energies, the positions of the corresponding LDOS peaks caused by interaction with halogens also shift in energy.

Let us discuss the evolution of the electron energy spectrum of the β2–GaAs (001)–(2 × 4) surface upon halogen adsorption using iodine as an example (Fig. 7). It can be seen that, at the T_1 site, there is a partially filled band, which is split from the top of the valence band. In this case, the local DOSs of gallium and arsenic atoms have a peak at the Fermi level (Fig. 6a). Such a tendency also takes place upon adsorption at the bridge D site above the surface dimers. It should be noted that, upon the adsorption of iodine at the H_3 and T_4 sites, such a band changes its bending, but is incompletely split from the valence states (Fig. 7). Upon the interaction of iodine with the subsurface gallium atom at the T_2' and even the T_3 site, the valence-band top is depleted, as was observed in the case of halogen adsorption at a cation-stabilized surface at top sites above dimerized and nondimerized gallium atoms ($M_1 - M_3$) [6].

3.3. Effect of Halogens on the Binding Energy of Surface Atoms

To estimate the effect of halogens on the energy of binding of arsenic and gallium atoms to the substrate, we calculated the total energies of systems with removed arsenic atoms of the surface and subsurface layers, as well as with removed gallium atom of the second layer at the missing row edge. Then, we calculated the energies of structures with Ga and As monohalides removed from the semiconductor surface with halogens adsorbed at the T_1, T_1', and T_2' sites. The binding energies of halogens in both top sites above arsenic dimer atoms and in the T_2' site above the gallium atom are listed in Table 3 together with the calculated energies of the binding of corresponding monohalides to the β2–GaAs (001)–(2 × 4) surface. It can be seen that, for all sites above arsenic atoms (T_1 and T_1'), the binding energy of monohalide to the substrate exceeds the binding energy of halogen adatom to the surface. It is worth noting that, at the top T_1 site, breakage of the dimer bond is not observed because of halogen adsorption, but the length of the bond between the dimer arsenic atom and gallium atoms of the second layer is increased by 0.17–0.24 Å for fluorine and by 0.15–0.20 Å upon iodine adsorption. Similarly, the length of the bond between the arsenic dimer atom of the third layer and gallium atoms in the forth layer is increased by ~0.15 Å for adsorption at the T_1' site. This means that, at low concentrations, the desorption of halogen occurs more easily than the desorption of arsenic halides. In con-

Table 3. Energies of the binding of halogens and corresponding monohalides to the β2–GaAs (001)–(2 × 4) surface and variation in energy ΔE_b of the binding of Ga and As surface atoms to the surface

β2–GaAs (001)–(2 × 4)		E_b			ΔE_b		
		T_1	T_1'	T_2'	T_1	T_1'	T_2'
F	E_b(monohalide-surface)	4.27	5.01	2.81	0.87	0.65	0.95
	E_b(halogen-surface)	3.70	4.01	4.77			
Cl	E_b(monohalide-surface)	4.30	4.88	2.92	0.86	0.69	0.92
	E_b(halogen-surface)	1.93	2.27	2.89			
Br	E_b(monohalide-surface)	4.39	–	2.94	0.83	–	0.91
	E_b(halogen-surface)	1.78	–	2.66			
I	E_b(monohalide-surface)	4.45	–	2.99	0.81	–	0.90
	E_b(halogen-surface)	1.18	–	1.79			

trast, upon fluorine adsorption at the T_2' position, gallium halide is more weakly bonded to the surface than the fluorine adatom (Table 3). In this case, GaF desorption can occur under normal conditions. The difference between the chlorine and gallium-chloride binding energies is minimal (~0.03 eV) and lies at the calculation-accuracy limit. Obviously, as in the previous case, the desorption of GaCl molecules can occur. It is worth noting that upon fluorine and chlorine adsorption at the T_2' site, the length of the bond between the surface dimer arsenic atom and gallium at the missing row edge also increases by ~0.2 Å and becomes longer than the sum of the arsenic and gallium covalent radii. As the electronegativity of the halogens is decreased, the difference in the binding energies between their adatoms and gallium halides increases; therefore, halogen desorption requires additional energy.

The weakening of the surface-atom binding ΔE_b caused by halogen adsorption was calculated as the difference between the binding energies of corresponding gallium (arsenic) atoms on a pure surface and on a surface with adsorbed halogen. The calculated decrease in the binding energy of surface atoms due to halogen adsorption at the three sites averaged over three bonds with nearest atoms is listed in Table 3. As on a cation-stabilized surface with the $\zeta - (4 \times 2)$ reconstruction, the formation of a bond between halogen and any surface and subsurface atom, depending on the adsorption site, leads to a decrease in the energy of its binding to the substrate; in this case, the bonds weaken appreciably for gallium atoms. The ΔE_b value slightly decreases in the series F–Cl–Br–I for both sites above gallium and above arsenic.

Thus, the interaction between halogens and a gallium atom at the missing row edge can make arsenic orbitals more reactive due to both charge transfer to gallium atoms and to a significant increase in the distance between these atoms and the bond break, which allows halogen atoms to also become bonded with surface arsenic atoms; i.e., the surface becomes disordered. Since the energies of fluorine, chlorine, and bromine atoms binding with arsenic atoms are also rather high, upon heating the substrate with these adsorbates, one can observe the desorption of the formed halides. At the same time, the low iodine binding energies on the As-stabilized GaAs (001) surface allow us to assume that the surface is passivated upon iodine adsorption. As the temperature is increased, iodine–arsenic bonds break earlier than arsenic–substrate ones. This was discussed in more detail in [9].

4. CONCLUSIONS

Using the projected augmented-wave method, we calculated halogen adsorption at an As-stabilized GaAs (001) surface with the β2–(2 × 4) reconstruction. We determined the preferred sites of halogen adsorption on this surface. It was shown that, within the submonolayer limit, halogens prefer to form bonds with a gallium atom of the second layer at the missing row edge at the T_2' site. The binding is of pronounced ionic type; in this case, the charge transferred to the halogen adatom is about 0.6–0.65*e* and increases with halogen electronegativity. Analysis of the charge-density distribution showed that gallium acquires the charge necessary for forming a stable bond with the nearest surface arsenic dimer atoms. Calculation of the electron energy spectra and local densities of states showed that upon halogen adsorption one can observe the depletion of halogen states that form the top of the valence band and are mainly arsenic states. According to the estimated variation in the substrate-atom binding energy due to interaction with halogens, the weakening of the bonds between gallium atoms above which halogen is adsorbed and the nearest arsenic atoms averaged over all bonds is ~0.90–0.95 eV. It was established that the energies of monohalide binding to the substrate are lower than the halogen-adatom bind-

ing energy for fluorine, but higher by 0.28 eV for bromine. At the same time, these values are nearly the same for chlorine. Since the binding energies for atoms above arsenic sites are fairly high, these halogens can also form bonds with arsenic, which is indicative of surface disordering and consistent with the experiment. In addition, halogens prefer to be adsorbed at the lower terrace of the missing row rather than above arsenic surface dimers, which also agrees well with the experiment [12]. A decrease in the binding energy of subsurface atoms and a slight increase in the interatomic distances are characteristic of the first stage of semiconductor etching, which can occur due to F, Cl, and Br. At the same time, less electronegative iodine is bonded to the substrate much weaker than GaI. Despite the significant charge transfer to iodine, as well as to the other halogens, there are no prerequisites for etching and iodine apparently passivates the surface. In general, the established trends in halogen adsorption at cation- [6–9] and anion-stabilized surfaces account for the experimental results reported in [10–12].

ACKNOWLEDGMENTS

This study was supported by the Russian Foundation for Basic Research, project no. 13-02-98017r_a and the Mendeleev Scientific Foundation of Tomsk State University, project no. 8.1.02.2015.

Numerical calculations were performed using the SKIF-Cyberia Supercomputer at Tomsk State University.

REFERENCES

1. W. Mönch, *Semiconductor Surfaces and Interfaces* (Springer, Berlin, 1995).
2. W. G. Schmidt, Appl. Phys. A **75**, 89 (2002).
3. S.-H. Lee, W. Moritz, and M. Scheffler, Phys. Rev. Lett. **85**, 3890 (2000).
4. W. C. Simpson and J. A. Yarmoff, Ann. Rev. Phys. Chem. **47**, 527 (1996).
5. S. Mirbt, N. Moll, A. Kley, E. Pehlke, and M. Scheffler, Surf. Sci. **422**, L177 (1999).
6. A. Bakulin, S. Eremeev, O. Tereshchenko, E. Chulkov, and S. Kulkova, IOP Conf. Ser.: Mater. Sci. Eng. **23**, 012015 (2011).
7. A. V. Bakulin, C. E. Eremeev, O. E. Tereshchenko, and S. E. Kulkova, Semiconductors **45**, 21 (2011).
8. A. V. Bakulin, S. E. Kulkova, S. V. Eremeev, and O. E. Tereshchenko, J. Phys. Chem. C **118**, 10097 (2014).
9. O. E. Tereshchenko, S. V. Eremeev, A. V. Bakulin, and S. E. Kulkova, JETP Lett. **91**, 466 (2010).
10. W. K. Wang, W. C. Simpson, and J. A. Yarmoff, Phys. Rev. Lett. **81**, 1465 (1998).
11. W. K. Wang, W. C. Simpson, and J. A. Yarmoff, Phys. Rev. B **61**, 2164 (2000).
12. Y. Liu, A. J. Komrowski, and A. C. Kummel, J. Chem. Phys. **110**, 4608 (1999).
13. P. E. Blöchl, Phys. Rev. B **50**, 17953 (1994).
14. G. Kresse and D. Joubert, Phys. Rev. B **59**, 1758 (1999).
15. G. Kresse and J. Hafner, Phys. Rev. B **47**, 558 (1993).
16. G. Kresse and J. Furthmüller, Comput. Mater. Sci. **6**, 15 (1996).
17. J. P. Perdew, K. Burke, and M. Ernzerhof, Phys. Rev. Lett. **77**, 3865 (1996).
18. S. M. Lee, S.-H. Lee, and M. Scheffler, Phys. Rev. B **69**, 125317 (2004).
19. D. R. Lide, *CRC Handbook of Chemistry and Physics* (CRC, Boca Raton, FL, 1996).
20. K. Shiraishi and T. Ito, Jpn. J. Appl. Phys. **37**, L1211 (1998).
21. H. J. Monkhorst and J. D. Pack, Phys. Rev. B **13**, 5188 (1976).
22. W. G. Schmidt and F. Bechstendt, Phys. Rev B **54**, 16742 (1996).
23. S. E. Kulkova, S. V. Eremeev, A. V. Postnikov, and I. R. Shein, J. Exp. Theor. Phys. **104**, 590 (2007).
24. N. Moll, A. Kley, E. Pehlke, and M. Scheffler, Phys. Rev. B **54**, 8844 (1996).
25. S. Q. Wang and H. Q. Ye, Phys. Rev. B **66**, 235111 (2002).
26. S. Zh. Karazhanov and L. C. Lew Yan Voon, Semiconductors **39**, 161 (2005).
27. J. E. Northrup and S. Froyen, Mater. Sci. Eng. B **30**, 81 (1995).
28. W. G. Schmidt, S. Mirbt, and F. Bechstedt, Phys. Rev. B **62**, 8087 (2000).
29. C. Hogan, D. Paget, Y. Garreau, M. Sauvage, G. Onida, L. Reining, P. Chiaradia, and V. Corradini, Phys. Rev. B **68**, 205313 (2003).
30. G. Henkelman, A. Arnaldsson, and H. Jónsson, Comput. Mater. Sci. **36**, 254 (2006).

Translated by E. Bondareva